

Fast Iterative Algorithms for Total Variation Based Multiplicative Noise Removal Model

¹Noor Badshah, ²Asmat Ullah, ³Mushtaq Ahmad Khan
 Department of Basic Sciences, UET Peshawar, Pakistan

Abstract: This paper presents fast iterative algorithms for solution of PDEs arisen from minimization of multiplicative noise removal model [14]. This model may be regarded as an improved version of the Total Variation (TV) de-noising models. For the TV and the multiplicative noise removal models, their associated Euler-Lagrange equations are highly nonlinear Partial Differential Equations (PDEs). For this model a very slow explicit time marching method has been reported. The main contribution we present in this paper is the implementation of the fixed point, semi-implicit and additive operator splitting schemes which do not yield good results. Consequently a fast and efficient multi-grid method with AOS as smoother is developed. Numerical experiments are presented to show the good performance of the fast multi-grid algorithm.

Key words. Synthetic Aperture Radar (SAR), Total Variation (TV)-based noise reduction, AOS (Additive Operator Splitting), Multi-Grid (MG), BV-Bounded Variation.

I. Introduction

Image de-noising is an inverse problem encountered in a wide variety of image processing fields [10, 21,14]. Multiplicative noise (speckle) is one of the more complex image noise. It is signal independent, non-Gaussian and spatially dependent. It appears in various image processing applications e.g., in Synthetic Aperture Radar (SAR), Ultrasound imaging or in connection with blur in electronic microscopy, single particle emission computed tomography (SPECT) and Positron Emission Tomography (PET). Many approaches have been proposed to tackle this problem. Among the famous ones are wavelets approaches, stochastic approaches, and variational approaches which is presented by Rudin, Osher and Fatemi (ROF) [16], it become evident that the variational approaches to the image de-noising problem can yield often excellent results. There exist several variational approaches concerned to multiplicative de-noising models.

The first TV-based multiplicative noise removal model was introduced by Rudin et al (RLO-model) [15] which used a constrained optimization approach with two Lagrange multipliers. Multiplicative de-noising model (AA-model) with a fitting term obtained from a MAP (Maximum a Posteriori) was presented by Aubert and Aujol [6, 1]. Shi and Osher [16, 14] adopted the data term of the AA-model and replace the regularizer $TV(\phi)$ by $TV(\log \phi)$ and letting $w = \log \phi$, they derived the strictly convex TV model (SO-model) [5]. Similarly with SO-model, Bioucas and Figueiredo converted the multiplicative model into an additive one by taking logarithms and introduced Bayesian type variational model [14]. Steidl and Teuber [14, 25] presented a variational model consisting of the 1-divergence as data fitting term and the TV-semi-norm as regularizer. A variational model involving curve let coefficients for cleaning multiplicative Gamma noise was introduced in [14].

II. Variational Model

According to [14] by applying the Total Variational (TV) approach, a functional well adapted to the removing of multiplicative noise is given by:

$$\min_{\phi} \left\{ \int_{\Omega} \left(\log \phi + \frac{f}{\phi} \right) dx + \eta_1 \int_{\Omega} |D\phi| + \eta_2 \int_{\Omega} \frac{|D\phi|}{\phi} \right\} \quad (1)$$

Where, the first term is the image fidelity term which measures the violation of the relation between ϕ and the observation f . The last two terms are the regularization terms, where η_1, η_2 are regularization parameters. The formal Euler-Lagrange equation [14] for any solution of functional (1) is as follows.

$$-\left(\frac{\eta_1 + \eta_2}{\phi} \right) \nabla \left(\frac{\nabla \phi}{\sqrt{|\nabla \phi|^2 + c}} \right) + \frac{\phi - f}{\phi^2} = 0, \quad \text{in } \Omega$$

$$\frac{\partial \phi}{\partial n} = 0 \quad \text{on } \partial \Omega \quad (2)$$

Since $\phi > 0$, then the Euler-Lagrange equation of minimizing can be rewritten equivalently as:

$$-\nabla \cdot \left(\frac{\nabla \phi}{\sqrt{|\nabla \phi|^2 + c}} \right) + \frac{\phi - f}{\phi(\eta_1 \phi + \eta_2)} = 0, \quad \text{in } \Omega$$

$$\frac{\partial \phi}{\partial n} = 0, \quad \text{on } \partial \Omega \tag{3}$$

Let $\tilde{\lambda} = \tilde{\lambda}(\phi) = \frac{1}{\phi(\eta_1 \phi + \eta_2)}$. Then equation (3) can be rewritten as

$$-\nabla \cdot \left(\frac{\nabla \phi}{\sqrt{|\nabla \phi|^2 + c}} \right) + \tilde{\lambda}(\phi - f) = 0, \quad \text{in } \partial \Omega \tag{4}$$

with the Neumann adiabatic condition along the boundary of the image domain. Notice that $\tilde{\lambda} > 0$, since $\phi > 0$. Equation (4) can be expressed in operator notation:

$$L(\phi)\phi = \tilde{\lambda}(\phi)f \tag{5}$$

where $L(\phi)$ is the linear diffusion operator whose action on a function χ is given by:

$$L(\phi)x = -\nabla \cdot \left(\frac{\nabla x}{\sqrt{|\nabla \phi|^2 + c}} \right) + \tilde{\lambda}(\phi)x \tag{6}$$

The fixed point iteration is then

$$L(\phi^{(n)})\phi^{(n+1)} = \tilde{\lambda}(\phi^{(n)})f, n = 0, 1, 2, \dots \tag{7}$$

Finite difference method [12, 7, 4], is used commonly for discretization of Partial Differential Equation (PDE). Equation (5) can be approximately computed by the first order accurate finite difference schemes described as follows [15, 14].

$$\Delta_x^\pm = \pm[\phi_i \pm 1, j - \phi_i, j], \Delta_y^\pm = \pm[\phi_i \pm 1, j - \phi_i, j] \tag{8}$$

$$|\Delta_x(\phi_{i,j})|_c = \sqrt{\Delta_x^+(\phi_{ij})^2 + (m[\Delta_y^+(\phi_{ij}), \Delta_y^-(\phi_{ij})])^2} + \epsilon, \tag{9}$$

$$|\Delta_y(\phi_{i,j})|_c = \sqrt{\Delta_x^+(\phi_{ij})^2 + (m[\Delta_x^+(\phi_{ij}), \Delta_x^-(\phi_{ij})])^2} + \epsilon \tag{10}$$

Where, $m(a, b) = (\text{sign}(a) + \text{sign}(b))/2, \min(|a|, |b|)$. Here, we denote the space step size by $h = 1, \epsilon > 0$. These schemes yield approximate form of equation (6).

$$L(\phi)x \approx \left(\Delta_x^- \left(\frac{\Delta_x^+ x}{|\Delta_x \phi|_c} \right) \right) + \left(\Delta_y^- \left(\frac{\Delta_y^+ x}{|\Delta_y \phi|_c} \right) \right) + \tilde{\lambda}(\phi)x \tag{11}$$

The matrix operators L , are symmetric and positive definite and sparse. Following experimental results will illustrate the performance of the numerical scheme.

III. Numerical Methods

Explicitly time marching methods have been applied for solving TV-image models [19], due to their simplicity but as it are conditionally stable. Therefore, we use the semi-implicit and additive splitting which are unconditionally stable to solve equation (4) with an artificial time step Δt i.e the following problem:

$$\phi_t = -\nabla \cdot \left(\frac{\nabla \phi}{\sqrt{|\nabla \phi|^2 + \epsilon}} \right) + \tilde{\lambda}(\phi - f), \quad \text{in } \Omega \tag{12}$$

with the Neumann adiabatic condition along the boundary of the image domain. Where:

$\tilde{\lambda} = \tilde{\lambda}(\phi) = \frac{1}{\phi(\eta_1 \phi + \eta_2)}$. The grid-point (i, j) is located at

$$(x_i, y_j) = \left(a + \frac{(2i-1)h}{2}, c + \frac{(2j-1)k}{2} \right), 1 \leq i \leq m_1, 1 \leq j \leq m_2$$

The value of f at each grid (i, j) is denoted by $f_{(i,j)}$. where as: $h = \frac{b-a}{m_1}$, $k = \frac{d-c}{m_2}$ are the grid spacings in the x,y-directions.

3.1.Semi-Implicit Scheme

Refer to [3,20], at time $t_{n=n\Delta t}$ denote $\phi_{i,j}^n = \phi(t_n, x_i, y_j)$ an approximation of $\phi(t, x, y)$ and using equation (4-12).we obtain the following linearized equation through semi-implicitness is given as:

$$\frac{\phi_{i,j}^{n+1} - \phi_{ij}^n}{\Delta t} = \Delta_x^- \left[\frac{\Delta_x^+ \phi_{i,j}^{n+1}}{\sqrt{((\Delta_x^+ \phi_{i,j}^{n+1} / h)^2 + (\phi_{ij+1}^n - \phi_{i,j-1}^n / 2k)^2)}} \right] + \Delta_y^- \left[\frac{\Delta_x^+ \phi_{i,j}^{n+1}}{\sqrt{((\phi_{i+1,j}^n - \phi_{i-1,j}^n / 2h)^2 + (\Delta_y^+ \phi_{i,j}^{n+1} / k)^2)}} \right] + \tilde{\lambda}(f_{i,j} - \phi_{i,j}^{n+1}) \tag{13}$$

Denoting the coefficients of $\phi_{i+1,j}^{n+1}, \phi_{i-1,j}^{n+1}, \phi_{i,j+1}^{n+1}, \phi_{i,j-1}^{n+1}, \phi_{i,j-1}^{n+1}$ by A_1, A_2, A_3, A_4 , respectively.

We get the following system of linear equations.

$$\left[1 + \Delta t \tilde{\lambda} + A_1, A_2, A_3, A_4 \right] \phi_{i,j}^{n+1} = \phi_{i,j}^n + \Delta t \left[A_1 \phi_{i+1,j}^{n+1} + A_2 \phi_{i-1,j}^{n+1} + A_3 \phi_{i,j+1}^{n+1} + A_4 \phi_{i,j-1}^{n+1} \right] + \Delta t \tilde{\lambda} f_{ij} \tag{14}$$

Which may be solved by an iterative method as a direct solution can be expensive for images of large size.

3.2 Additive Operator Scheme

It is already stated that semi-implicit scheme is unconditionally stable but it is can allow large time steps. Its main drawback is the computational cost of the associated linear systems for large images. Hence, we need an iterative method which is unconditionally stable, time efficient and easy to implement to solve the PDEs. So we introduce the AOS scheme [3, 18], which provides an equally accurate and yet more efficient SI-scheme by splitting the two dimensional spatial operator into two separate 1-dimensional space discretizations and then applying 1-dimensional SI-scheme in turns. Then two tri-diagonal systems are solved per iteration than a band five system.

Following equation (12) we have

$$\phi_t = -\tilde{\mu} \nabla \left(\frac{\nabla \phi}{\sqrt{|\nabla \phi|^2 + \varepsilon}} \right) + \phi - f, \quad \text{in } \Omega \tag{15}$$

With the Neumann adiabatic condition along the boundary of the image domain. Where $\tilde{\mu} = \tilde{\mu}(\phi) = \phi(\eta_1 \phi + \eta_2)$. Consider equation (15) in the form

$$\frac{\phi_i^{n+1} - \phi_i^n}{\partial t} = -\tilde{\mu} \nabla \cdot (P \nabla u) + \phi - f = -\tilde{\mu} (\partial_x (P \partial_x \phi) + \partial_y (P \partial_y \phi)) + \phi_i^{n+1} - f_i \tag{16}$$

Where $P = \frac{1}{\sqrt{|\nabla \phi|^2 + \varepsilon}}$

$$\begin{aligned} \frac{\phi_i^{n+1} - \phi_i^n}{\partial t} &= -\tilde{\mu} \left[\left(\frac{P_i^n + P_{i+1}^n}{2} \right) (\phi_{i+1}^{n+1} - \phi_i^n) - \left(\frac{P_i^n - P_{i-1}^n}{2} \right) (\phi_{i+1}^{n+1} - \phi_{i-1}^{n+1}) \right] + \phi_i^{n+1} - f_i \\ \Rightarrow \phi_i^{n+1} - \phi_i^n &= -\tilde{\mu} \partial t \left[\left(\frac{P_i^n + P_{i+1}^n}{2} \right) (\phi_{i+1}^{n+1} - \phi_i^n) - \left(\frac{P_i^n - P_{i-1}^n}{2} \right) (\phi_{i+1}^{n+1} - \phi_{i-1}^{n+1}) \right] + \partial t (\phi_i^{n+1} - f_i) \\ \phi_i^{n+1} &= \phi_i^n - \tilde{\mu} \partial t [c_1 \phi_{i+1}^{n+1} - c_2 \phi_{i-1}^{n+1} + c_3 \phi_i^{n+1}] + \partial t \phi_i^{n+1} - \partial t f_i \end{aligned} \tag{17}$$

where $c_1 = \frac{P_i^n + P_{i+1}^n}{2}, c_2 = \frac{P_{i-1}^n + 2P_i^n + P_{i+1}^n}{2}, c_3 = \frac{P_i^n - P_{i-1}^n}{2}$

After we solve the system of equations (17) in the x-direction, we then solve a similar system in the y-direction before averaging the two solutions. In matrix notation the process can be written as

$$(1 - 2\partial t A_l(\phi^n)) \phi_i^{n+1} = f^n, \text{ for } l=1,2 \text{ and } \phi_i^{n+1} = \frac{1}{2} \sum_{l=1}^2 \phi_i^{n+1} \tag{18}$$

Where I is the identity matrix, and A_l for $l = 1, 2$ are tri-diagonal matrices derived from (18).

IV. Multi-Grid Method

It is known that convergence rate is very slow when using standard numerical optimization techniques. Therefore, we introduce the multi-grid algorithm to solve this system. Also, we need an iterative solver that eliminates the high frequency components of the residual quickly and efficiently. Iterative algorithms with this property are called smoothers. In

This paper, we introduce the Additive Operator Splitting method as smoother. Multi-Grid methods have been recently developed. It was first introduced by Brandt [2, 13, 11, 3, 22, 23, 8]. Unlike the conventional numerical schemes, the multi-grid algorithm can solve non-linear elliptic PDEs with non-constant coefficients with hardly any loss in efficiency.

The equation (4) at grid point (i, j) is given as:

$$\phi_{i,j} - \phi_{i,j} (\eta_1 \phi_{i,j} + \eta_2) \left[\nabla \cdot \left(\frac{\nabla \phi_{i,j}}{\sqrt{|\nabla \phi_{i,j}|^2 + c}} \right) \right] = f_{i,j} \tag{19}$$

with the Neumann boundary conditions

$$\phi_{i,0} = \phi_{i,1}, \phi_{i,m+1} = \phi_{i,m}, \phi_{0,j} = \phi_{1,j}, \phi_{n+1,j} = \phi_{n,j}.$$

4.1. The choice of Smoothers and the overall Multi-Grid Algorithm

Several iterative methods can be applied as smoothers for multi-grid scheme like fixed point iteration, JAC, and Gauss Seidal schemes etc. Here AOS is given as smoother which work well with the standard non-linear multi-grid method [24].

4.1.1. Smoother S_1

Iterative solver that smooth the high frequency components of the residual quickly and efficiently. Iterative algorithms with this property are called smoothers. For linear problems with smooth coefficients, it is well-known that Gauss-Seidel, Jacobi and SOR methods are good smoothers. For non-linear problems, however it is not an easy task to implement a good one. In this work, Additive Operator Splitting (AOS) has been used as smoother

which yield our desired results in de-noising the images.

4.1.2. The Full Approximation Scheme (Multi-Grid Method)

System of non-linear equations is denoted by:

$$N^h \phi^h = f^h \tag{20}$$

Where N^h is non-linear operator ϕ^h and f^h are grid functions on an $m_1 \times m_2$ grid Ω^h with grid spacing (h, k) . The $m_1 \times m_2$ cell centered grid by Ω^{2h} which results from the standard coarsening of Ω^h . If ϕ^h is an approximation to the solution of equation (19) define the error in ϕ^h by $e^h = \phi^h - \phi^h$ and the residual by $r^h = f^h - N^h \phi^h$. By the use of coarse grid correction the error can be smoothed by the use of any iterative method. For multi-grid scheme we use the interpolation and restriction operators for transferring the grid functions between Ω^h and Ω^h and Ω^{2h} . Refer to [9, 17], we have

4.1.3. Restriction

$$R_h^{2h} \phi^h = \phi^{2h} \tag{21}$$

Where, $1 \leq i \leq \frac{m_1}{2}, 1 \leq j \leq \frac{m_2}{2}$

$$\phi_{(i,j)}^{2h} = \frac{1}{4} [\phi_{2i-1,2j-1}^h + \phi_{2i-1,2j}^h + \phi_{2i,2j-1}^h + \phi_{2i,2j}^h]$$

4.1.4. Interpolation

$$R_{2h}^h \phi^{2h} = \phi^h \tag{22}$$

$$\phi_{(2i,2j)}^h = \frac{1}{16} [9\phi_{(i,j)}^{2h} + 3(\phi_{(i+1,j)}^{2h} + \phi_{(i,j+1)}^{2h}) + \phi_{(i+1,j+1)}^{2h}]$$

$$\begin{aligned}\varphi_{(2i-1,2j)}^h &= \frac{1}{16} \left[9\varphi_{(i,j)}^{2h} + 3(\varphi_{(i-1,j)}^{2h} + \varphi_{(i,j+1)}^{2h}) + \varphi_{(i-1,j+1)}^{2h} \right] \\ \varphi_{(2i,2j-1)}^h &= \frac{1}{16} \left[9\varphi_{(i,j)}^{2h} + 3(\varphi_{(i+1,j)}^{2h} + \varphi_{(i,j-1)}^{2h}) + \varphi_{(i+1,j-1)}^{2h} \right] \\ \varphi_{(2i-1,2j-1)}^h &= \frac{1}{16} \left[9\varphi_{(i,j)}^{2h} + 3(\varphi_{(i-1,j)}^{2h} + \varphi_{(i,j-1)}^{2h}) + \varphi_{(i-1,j-1)}^{2h} \right]\end{aligned}$$

4.1.5. The Multi-Grid Algorithm

To solve equation (19) our multi-grid algorithm which is known as Full Approximation Scheme (FAS) may be summarized as follows [3].

Algorithm-1

Following multi-grid parameters may be applied:

ν_1 Pre-smoothing steps on each level

ν_2 Post-smoothing steps on each level ℓ the multilevel grids cycles on each level ($\ell = 1$ for V-cycling $\ell = 2$ for W-cycling) here we take the V-cycle with $\ell = 1$

1. FAS Multi-grid cycle

$$\hat{\phi}^h \leftarrow \text{FASCY } C(\hat{\phi}^{2h}, f^{2h}, \text{iter}, \nu_1, \nu_2, \ell)$$

2. If Ω is the coarsest grid, then solve (20) using time marching technique of [3], and then stop. Else implement a smoother

$$\phi^h \leftarrow \text{Smoother } \nu^1(\hat{\phi}^h, f^h, \nu_1), \text{ (Pre-smoothing step)}$$

3. Restriction

$$\hat{\phi}^{2h} = I_h^{2h} \hat{\phi}^h, \quad \hat{\phi}^{2h} = \hat{\phi}^{2h} f^{2h} = I_h^{2h} (f^h - N^h \hat{\phi}^h) + N^{2h} \hat{\phi}^{2h}$$

$$4. \quad \hat{\phi}^{2h} \leftarrow \text{FASCY } C_\ell(\hat{\phi}^{2h}, f^{2h}, \text{iter}, \nu_1, \nu_2, \ell) + N^{2h} \hat{\phi}^{2h}$$

5. Interpolation

$$\hat{\phi}^h \leftarrow \hat{\phi}^h + I_{2h}^h (\hat{\phi}^{2h} - \hat{\phi}^{2h})$$

$$6. \quad \hat{\phi}^h \leftarrow \text{smoother } \nu^2(\hat{\phi}^h, f^h, \nu_2) \quad \text{(Post-smoothing)}$$

V. Experimental Results

In this paper, experiments are carried out on gray scale images of different sizes (pixels) and ranges from [0 127] to [0 2047] with multiplicative noise/speckle. Experimental results are given to demonstrate the performance of multi-grid with AOS (MG), with other numerical schemes likely, semi-implicit, fixed point and additive operator splitting (AOS) schemes. Figure1, shows test images for de-noising namely Problem1, Problem2 and Problem3. The de-noised images are shown in figure2, figure3, figure4 for visual comparison. Figure2 consists of problem1, which is de-noised by semi-implicit, fixed Point, additive operator splitting schemes, and multi-grid algorithms. Parameters used are $\eta_1 = 15, \eta_2 = .003$. Figure3 shows problem2, restoration of image is made by semiimplicit method, fixed point iterative method, additive operator splitting scheme, and multi-grid algorithms with $\eta_1 = .005, \eta_2 = .0009$. Figure4 shows problem3, which is restored by semi-implicit, fixed Point, additive operator splitting scheme, and multi-grid algorithms with $\eta_1 = .003, \eta_2 = .0009$. In each case better performance of MG can be seen over other iterative schemes. In addition, from table1 one can see that multi-grid MG is more efficient and effective. It may be noted that for large images the multi-grid algorithm MG takes more time because for better de-noising results we apply large cycles of pre-smoothing and post-smoothing steps that is $\vartheta_1 = 17, \vartheta_2 = 27$. Furthermore, we gave the speed comparison of the four schemes which includes the number of iterations (It.) and the CPU time for the images of different sizes. Following abbreviations may be helpful for reading the given table which is given as under:

- SIM: Semi-Implicit Scheme
- FPIS: Fixed Point Iteration Scheme

- AOS: Additive Operator Splitting Scheme
- MG: AOS based multi-grid.

5.1. Test Images for De-noising

Following are the test images which will be used for de-noising throughout in this work, which are assigned names as Problem1, Problem2 and Problem3.

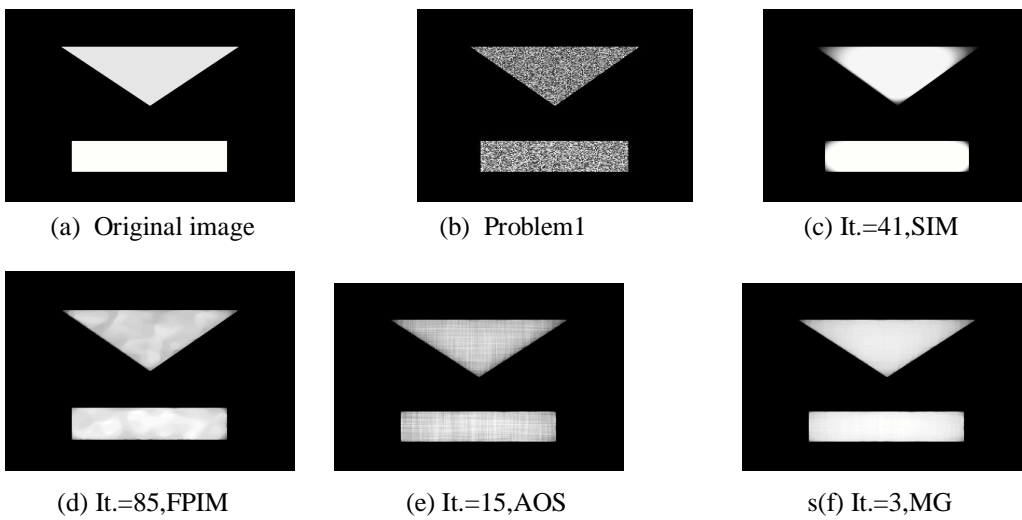


(a) Problem1

(b) Problem2

(c) Problem3

Figure.1 Test Images for de-noising



(a) Original image

(b) Problem1

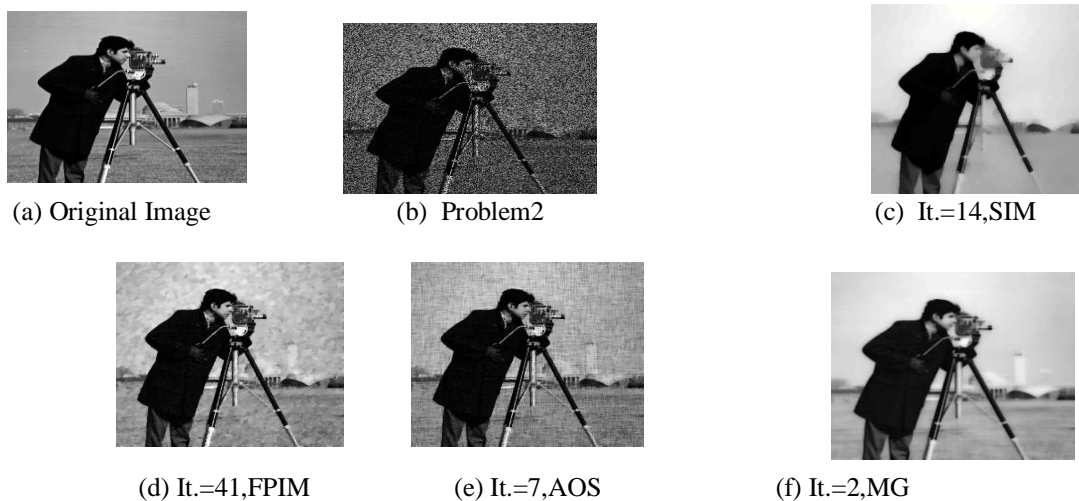
(c) It.=41, SIM

(d) It.=85, FPIM

(e) It.=15, AOS

(f) It.=3, MG

Figure.2 Problem1(256^2) denoised image by semi-implicit, fixed point, and additive operator splitting schemes with number of iterations=41, 85, 15 and multi-grid algorithm MG, with number of cycles=3, by choosing $\eta_1 = 15, \eta_2 = .0003$.



(a) Original Image

(b) Problem2

(c) It.=14, SIM

(d) It.=41, FPIM

(e) It.=7, AOS

(f) It.=2, MG

Figure.3 Problem1(256^2) denoised image by demi-implicit, fixed point, and additive operator splitting schemes with number of iterations=41, 85, 15 and multi-grid algorithm MG, with number of cycles=2, by choosing $\eta_1 = .005, \eta_2 = .0009$.

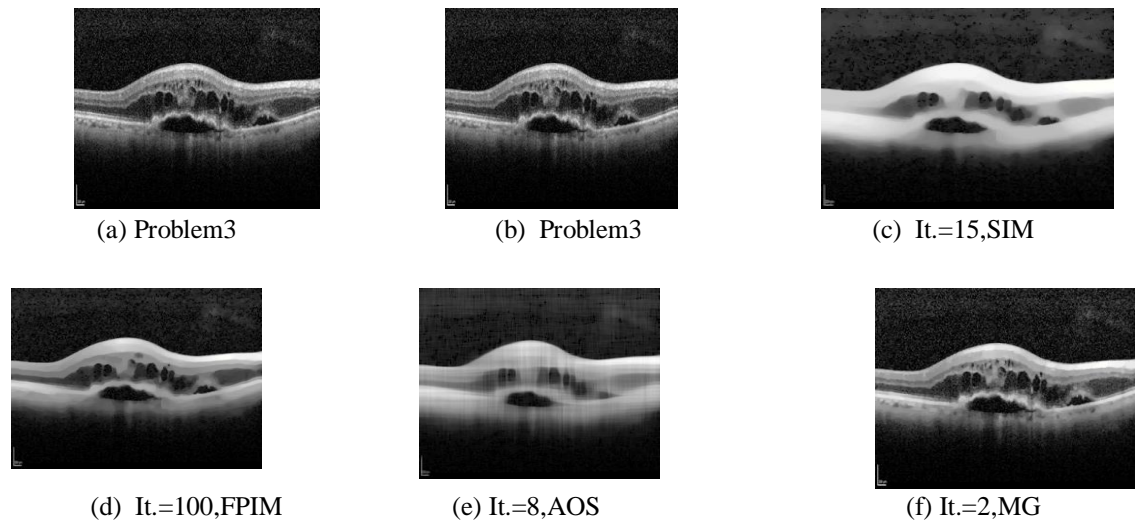


Figure.4 Problem1(256²) denoised image by demi-implicit, fixed point, and additive operator splitting schemes with number of iterations=15,100,8 and multi-grid algorithm MG, with number of cycles=2, by choosing $\eta_1 = .003, \eta_2 = .0009$.

Problem	Size	SIM		FPIS		AOS		MG	
		It.	CPU	It.	CPU	It.	CPU	It.	CPU
Problem1	128 ²	30	4	75	15	15	2	3	2
	256 ²	41	15	85	31	15	5	3	6
	512 ²	50	81	97	85	16	24	3	23
	1024 ²	59	411	109	195	19	124	3	88
	2048 ²	71	586	127	730	22	390	3	271

Problem2	128 ²	11	2	28	10	7	1	2	1
	256 ²	14	13	41	154	8	3	2	2
	512 ²	19	87	55	824	8	10	2	9
	1024 ²	25	827	69	1312	10	37	2	32
	2048 ²	31	2031	87	2528	13	158	2	112

Table.1 Comparison of semi-implicit scheme, fixed point iteration scheme, additive operator scheme and multi-grid scheme for speckle images of Problem1 (128² – 2048²) and Problem2 (128² – 2048²) with CPU-time and number of iterations.

VI. Peak Signal-to-Noise Ratio (PSNR)

We measure the quality of the restored image by the peak signal-to-noise ratio (PSNR) defined by

$$PSNR = 10 \log_{10} \left[\frac{(m_1 \times m_2) \max(\phi)^2}{\|u_0 - \phi\|^2} \right]$$

Where u_0 is the original image, ϕ is the restored image and $m_1 \times m_2$ is the size of the image.

Problem	Size	SIM	FPIS	AOS	MG
		PSNR	PSNR	PSNR	PSNR
Problem1	256 ²	19.05	14.54	19.37	19.69

Problem3	256 ²	24.03	20.23	25.67	25.89
----------	------------------	-------	-------	-------	-------

Table.2: It shows the Peak Signal-to-Noise Ratio (PSNR) results by semi-implicit, fixed point, additive operator splitting schemes and MG on gray level image of problem1 and problem3. From the table, we can see that the PSNR of the image restored by using MG is more than those restored by using the other schemes.

VII. Conclusion

In this paper, additive operator splitting method based multi-grid method for multiplicative noise/speckle suppression is presented. By applying the multi-grid algorithm, the technique has the advantage of speed of computation and effectiveness in de-noising the images over the standard iterative techniques of semi-implicit scheme, fixed point iteration scheme, and additive operator scheme. Future work will address multi-grid methods for other variational models and alternative multilevel methods. Furthermore, it is intended to apply mesh-free methods for PDEs arisen from minimization of variational models.

References

- [1] G. Aubert and J. F. Aujol, *A variational approach to removing multiplicative noise*, SIAM Journal on Applied Mathematics **68** (2008), no. 4, 925–946.
- [2] G. Aubert and P. Kornprobst, *Mathematical problems in image processing of applied mathematical sciences*, Springer, Berlin, Germany **147** (2002).
- [3] N. Badshah and K. Chen, *Multigrid method for the Chan-Vese model in variational segmentation*, Communications in Computational Physics **4** (2008), no. 2, 294–316.
- [4] N. Badshah and K. Chen, *On two multi-grid algorithms for modelling variational multi-phase image segmentation*, IEEE transactions on image processing **18** (2009), no. 5, 1097–1106.7 Conclusion 13
- [5] C.B. Burkhardt, *Speckle in ultrasound b-mode scans.*, IEEE Trans. Ultrasonic, **25** (1978), no. 1, 1–6.
- [6] V. Vasselis G. Sapiro C. Ballester, M. Bertalmio and J. Verera, *Filling in by joining interpolation of vector fields and grey levels*, IMA Technical Report, university of Minnesota **69** (2002), no. 7, 131–147.
- [7] Y. Liping C. Sheng, Y. Xin and S. Kun, *Total variation based speckle reduction using multigrid algorithm for ultrasound images.*, Springer-Verlag Berlin Heidelberg **36** (2005), no. 17, 245–252.
- [8] T. F. Chan and K. Chen, *On a nonlinear multi-grid algorithm with primal relaxation for the image total variation minimization*, SIAM J. Sci. Comput. **20** (2006), no. 13, 387–411.
- [9] R. Deriche, *Fast algorithms for low-level vision*, IEEE Transactions pattern Anal. Mach. Intell. **12** (1990), no. 9, 78–87.
- [10] X. Zeng F. Tian Z. Li G. Liu and K. Chaibou, *Speckle reduction by adaptive window anisotropic diffusion*, signal processing **89** (2009), no. 11, 233–243.
- [11] J. W. Goodman, *Some fundamental properties of speckle*, Journal of Opt. Soc. Am. **66** (1976), no. 6, 1145–1150.
- [12] D. C. Munson Jr and R. L. Visentin, *A signal processing view of strip-mapping synthetic aperture radar*, IEEE Transactions on acoustics, speech, and signal processing, **37** (1989), no. 12, 2131–2147.
- [13] R. Kikinis K. Krissian, C. F. Westin and K. G. Vosburgh, *Oriented speckle reducing anisotropic diffusion*, IEEE Transactions on image processing **16** (2007), no. 5, 142–155.
- [14] L. Xiao L. Huang and Z. H. Wei, *Multiplicative noise removal via a novel variational model*, EURASIP Journal on image and video processing **1135** (2010), no. 250768,768–782.
- [15] P. L. Lions L. I. Rudin and S. Osher, *Multiplicative denoising and deblurring theory and algorithms, in geometric level set methods in imaging, vision, and graphics, s.osher and n. paragios, ed.*, Springer, Berlin, Germany, (2003), 103–120.
- [16] S. Osher L. I. Rudin and E. Fatemi, *Non-linear total variation based noise removal algorithms*, Physica D **60** (1992), 259–268.
- [17] C. F. B. Loeza, *Fast numerical algorithms for high order pdes with application to image restoration techniques*, Ph.D. thesis, university of Liverpool, 2009.
- [18] P. Lin R. Glowinski and X. B. Pan, *An operator-splitting method for a liquid crystal model.*, comp. Phys. Comm. **152** (2003), no. 152, 242–252.
- [19] M.M. Crawford S. T. Acton, A.C. Bovik, *Anisotropic diffusion processing for image segmentation*, Proc. IEEE Int. Conf. Image Processing (ICIP-94), Austin **3** (1994), no. 478–482.
- [20] J. Shen, *On the foundation of vision modeling: I. weber's law and weberized tv restoration.*, Physica D **175** (2003), no. 3-4, 241–251.
- [21] J. Shi and S. Osher, *A nonlinear inverse scale space method for a convex multiplicative noise model.*, SIAM Journal on imaging sciences, **1** (2008), no. 3, 294–321.
- [22] C. W. Oosterlee U. Trottenberg and A. Schuller, *Multigrid*, Institute of Algorithms and scientific Computing (SCAI), GMD-German national Research center for IT, Germany (2001).
- [23] E. H. Weber, *De pulsu, resorptione, audita et tactu.*, in Annotationes anatomicae et Physio-logicae, Koehler, Leipzig, Germany (1834).
- [24] P. Wesseling, *An introduction to multi-grid methods*, Wiley, Chichester, 1992.
- [25] M. K. Ng, Y. M. Huang and Y. W. Wen, *A new total variation method for multiplicative noise removal.*, SIAM Journal on imaging sciences, **2** (2009), no. 1, 22–40.